  Bull. Chem. Soc. Jpn., 55, 1379—1386 (1982)

Internal Heavy Atom Effect on the T_1 States of Halogen-substituted Benzonitriles

Yoshinori Asahi and Noboru Hirota*,†

Department of Chemistry, Faculty of Science, Kyoto University, Kyoto 606

(Received August 22, 1981)

The magnetic and decay properties of the ortho-, meta-, and para-substituted benzonitriles have been investigated and the nuclear charge and the position dependences of the internal heavy atom effects are examined in detail. From the single crystal EPR studies spin densities at the halogen atoms (ρ_H) are found to be in the order $\rho_H(\text{para}) > \rho_H(\text{ortho}) > \rho_H(\text{meta})$, but $\rho_H(\text{meta})$ is found to be much larger than that expected from the spin distribution in benzonitrile. The changes in the ZFS on going from the chloro-substituted molecules to the bromo-substituted molecules correlate with ρ_H and are explained in terms of the second order effect of the spin orbit mixing with $^3\sigma\pi^*$ ($^3\pi\sigma^*$) and $^3n\pi^*$ states. In the para-substituted molecules the relative increases of the T_y sublevel decay rates (k_y) are much greater than those of the T_z sublevel decay rates (k_z). The dependence of the average decay rate, $1/2(k_y+k_z)$ on the atomic spin orbit coupling constant (ζ), is considerably larger than expected from the ζ^2 dependence. These results were discussed in connection with the closeness of the $^3\sigma\pi^*$ ($^3\pi\sigma^*$) states in bromine containing molecules. A correlation between the decay rate and ρ_H is observed and the factors affecting the position dependence are examined.

When a halogen atom is substituted into an aromatic molecule, drastic changes in the properties of a triplet state molecule are observed.[1] The magnitude of this so-called internal heavy atom effect depends on the nuclear charge of the substituent, the type of molecule and the position of substitution. The nuclear charge dependence has been investigated rather intensively and in the systems so far studied the magnitude of the effect appears to be roughly proportional to the squares of the atomic spin orbit coupling constant ζ of the substituent.[1-5] Although this dependence has been rationalized qualitatively on the basis of the spin orbit matrix elements between the T_1 state and the perturbing singlet states, further examination of this dependence, especially in connection with the decay rates of the spin sublevels, may be useful in clarifying the relative importance of the different decay mechanisms.

The magnitude of the internal heavy atom effect is also dependent on the type of molecule. For example, the effects of the bromine substitution on the zero field splitting (ZFS) and the decay rates of the substituted benzenes[6,7] are far greater than those of naphthalene.[8,9] As for the position dependence Miller *et al.*[4] found in naphthalene and phenanthrene that there is a correlation between the magnitude of the heavy atom effect on the decay rate and the spin density on the carbon to which the heavy atom is attached. However, the data on the position dependence are scarce and further investigation seems to be worthwhile.

In the present work we have studied the T_1 states of the halogen-substituted benzonitriles by means of zero field optically detected magnetic resonance (ZFODMR) and EPR in order to examine the above mentioned dependences further. The main motives of the present study are the following.

(1) Benzonitrile may be considered as a typical example of the substituted benzenes having quinoid structures in the T_1 states. Our previous EPR investigation[10] has shown that the spin densities on the para, ortho, and meta positions are 0.33, 0.12, and 0.007, respectively. Because of the large differences in the spin densities it was thought that the halogen-substituted benzonitriles might be suited to investigate the position dependence of the internal heavy atom effect in detail.

(2) Previous ODMR studies on the bromine containing substituted benzenes have indicated that $^3\sigma\pi^*$ ($^3\pi\sigma^*$) and $^3n\pi^*$ states are likely to be rather close to the T_1 states.[6,7] This may lead to a nuclear charge dependence which is very different from those found for the other aromatics previously.

(3) The previous works on the nuclear charge dependence were made using the total decay rate constants. However, since different perturbing states are involved in the decay processes of the different sublevels nuclear charge dependence may depend on the sublevel significantly.

Here we first discuss the spin densities on the halogen atoms from the analysis of the hyperfine structures and the zero field splittings. We then examine the factors which affect the nuclear charge and position dependences of the decay rates in detail and discuss the observed dependences in connection with the spin distributions and the energy separations between the T_1 states and the main perturbing states.

Experimental

Guest molecules investigated here are 4-, 3-, and 2-fluorobenzonitrile (FBN), 4-, 3-, and 2-chlorobenzonitrile (ClBN), and 4-, 3-, and 2-bromobenzonitrile (BrBN). Hereafter we use the abbreviations given in parentheses. 3FBN and 2FBN were purified by distillation under reduced pressure and the others were purified by recrystallization from ethanol followed by sublimation under vaccum. The host crystals used here are *p*-xylene (PX), *o*-xylene (OX), *m*-xylene (MX) which were purified by distillation under reduced pressure and 1,4-dibromobenzene (DBB) and 1,4-dichlorobenzene (DCB) which were purified by recrystallization from ethanol and extensive zone refining. The molecular structure, the axis system and the numbering of the carbon atoms of para-substituted benzonitriles are

† Also at Department of Chemistry, State University of New York at Stomy Brook, New York, 11794, U.S.A.

Table 1. Observed and calculated hyperfine coupling constants of 2- and 3-fluorobenzonitriles

2FBN					3FBN				
Spin density ($2P_x$)		Hfcc A_x/mT			Spin density ($2P_x$)		Hfcc A_x/mT		
	Calcd		Calcd[a]	Obsd		Calcd		Calcd[a]	Obsd
C1	0.3049				C1	0.3021			
C2	0.1233				C2	0.0815	H2	0.196	
C3	−0.0235	H3	0.056		C3	0.0074			
C4	0.3192	H4	0.766	0.77	C4	0.3402	H4	0.816	0.83
C5	0.0040	H5	0.009		C5	−0.0125	H5	0.030	
C6	0.0888	H6	0.213	0.54	C6	0.1162	H6	0.279	0.44
C7	−0.0387				C7	−0.0389			
N	0.2046			0.69	N	0.2001			0.70
F	0.0167	F	3.064	2.60	F	0.0031	F	0.385	2.00

a) Hfcc of H was calculated using the values of Q and A_x^d for triplet benzene,[14] and hfcc of F was calculated by the analytical evaluation of dipolar integral.[12]

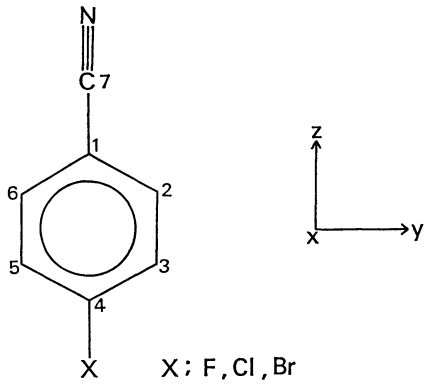

Fig. 1. Molecular structure, axis system, and numbering of the carbon atoms of the para-substituted benzonitriles.

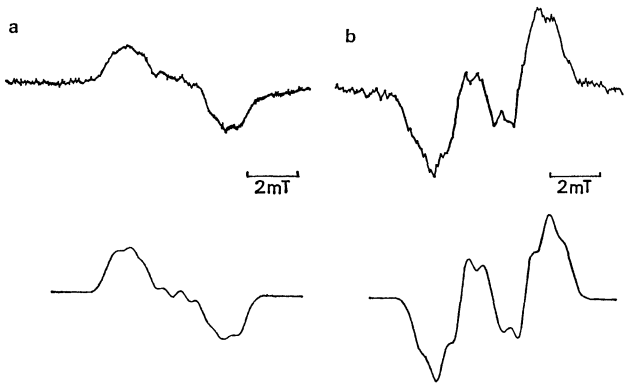

Fig. 2. Observed and simulated hyperfine structures when the applied field is perpendicular to the molecular plane.
(a): 3-Florobenzonitrile in DBB, (b): 2-fluorobenzonitrile in DBB. The upper spectra are experimental and the lower are simulated.

shown in Fig. 1.

The crystals were melt grown using the Bridgman method. When the host crystal was OX or MX, the solution containing a small amount of guest molecule was degassed by freeze-pump-thaw method and sealed in a 4 mm quartz tube. The sample mounted in the helical slow wave structure was cooled slowly to the liquid nitrogen temperature and was inserted rapidly into the helium cryostat. In other cases the crystals cut to the appropriate sizes were mounted in the helical slow wave structure in the ZFODMR experiments or on the acryl resin sample holder in the EPR experiments. The experimental setups and the procedure are essentially the same as those reported previously.[11,12]

Results and Disscussion

Hyperfine Splittings and Spin Distributions in the Halogen-substituted Benzonitriles. The spin densities in the T_1 state benzonitrile at the para, ortho, and meta positions were estimated to be 0.33, 0.12, and 0.007, respectively.[10] Halogen substitution, especially fluorine substitution, does not perturb the spin distribution of the parent molecule in the aromatic molecules such as naphthalene.[13] Fluorine or bromine substitution to benzonitrile at the para position also does not change the spin distribution much, although considerable spin delocalization of the unpaired electron into the halogen atom takes place.[12] The spin densities at the carbon 4 and the fluorine atom in 4FBN are 0.32 and 0.046, respectively.[12]

In Fig. 2 EPR spectra of 2FBN and 3FBN in DBB host taken with the applied field **B** perpendicular to the molecular plane are shown together with the simulated spectra. The fluorine splittings (A_x) estimated from the simulation are 2.6 mT for 2FBN and 2.0 mT for 3FBN. In the previous work on 4FBN[12] it was shown that a good agreement between the observed and calculated splittings was obtained using the molecular geometry of benzonitrile obtained from the bond orders calculated by the PPP UHF method for the T_1 state of benzonitrile. We have made similar calculations for 2FBN and 3FBN assuming the same geometries. The calculated A_x agrees reasonably well with the observed one in 2FBN, but the experimental value is far greater than the calculated one in 3FBN as shown in Table 1. This result seems to indicate that the structure of the T_1 state 3FBN is substantially different from that of benzonitrile. The normally used assumption[13] that the fluorine substitution does not perturb the spin distribution of

Table 2. Zero field splittings of halogen containing benzonitriles

System		ν_{00}/cm^{-1}	$\lvert D\rvert/cm^{-1}$	$\lvert E\rvert/cm^{-1}$
4BrBN	in PX	25766	0.168[a]	0.0129[a]
	in DBB	26202	0.156	0.0176
	in DCB	26235	0.157	0.0186
3BrBN	in MX	26535	0.160	0.0119
	MX doped	26095	0.148	0.0112
2BrBN	in OX	26295	0.183	0.0161
	OX doped	26286	0.153	0.0096
4ClBN	in PX	25799	0.135	0.0050
	in DBB		0.132	0.0045
	in DCB	26239	0.133	0.0058
	PX poped	25673	0.132	0.0042
3ClBN	MX doped	26041	0.134	0.0145
2ClBN	neat	26378	0.139	0.0133

a) Taken from Ref. 6.

the parent molecule appears to be no longer correct in the case of 3FBN. Nevertheless, the spin densities on the fluorine $2P_x$ orbitals are in the order $\rho(4FBN)>\rho(2FBN)>\rho(3FBN)$ following the order of the spin densities on the carbon atoms of the corresponding positions of benzonitrile.

In view of the fact that the delocalization of the unpaired electron into the bromine $4P_x$ orbital is greater than that into the fluorine $2P_x$ orbital, deviation from the benzonitrile structure may even be more serious in 3BrBN than in 3FBN.

Zero Field Splittings and the Contribution of Spin Orbit Coupling. It is known that the ZFS of the para-bromo-substituted benzenes are greatly affected by the second order effect of the spin orbit coupling.[6,7] We determined the magnitudes of the ZFS of the ortho-, meta-, and para-substituted benzonitriles from the microwave frequencies for the zero field ODMR transitions. From the previous EPR study[6] the relative ordering of the sublevels of 4BrBN are known to be $T_z>T_y>T_x$: Here, the z axis is parallel to the C–Br direction, the x axis is perpendicular to the molecular plane, and the y axis is perpendicular to the other two. For the ortho- and meta-substituted molecules the relative ordering of the zero field sublevels as well as the directions of the in-plane principal axes of the fine structure tensor are not known. In these cases we designate the sublevels $T_{z'}$, $T_{y'}$, and $T_{x'}$ from the top.

The ZFS of the halogen-substituted benzonitriles studied here are listed in Table 2. The ZFS of the bromo- and chloro-substituted molecules are substantially affected by the choice of the host crystal. However, if we compare the $|D|$ of the bromo-substituted molecules with those of the chloro-substituted molecules in the same host or in the X traps, the $|D|$ of the bromo-substituted molecules are always larger. This seems to indicate that the contribution of the second order effect of the spin orbit coupling is significant in both 2BrBN and 3BrBN.

The depression of the sublevel energy caused by the spin orbit mixing with the perturbing state p is given by[15,16]

$$\Delta E^1 = \sum_{p\neq T_1}\sum_{v}\frac{|\langle\Psi^0_{pv}|H_{so}|\Psi^0_{T_1 0}\rangle|^2}{E^0_{T_1 0}-E^0_{pv}}, \quad (1)$$

where $\Psi^0_{T_1 0}$ is the wave function of the sublevel i of the zeroth vibrational unperturbed T_1 state and Ψ^0_{pv} are of the zeroth order perturbing states. v stands for the vibrational states of the perturbing state. It was suggested that the spin orbit mixing with the $^3\sigma\pi^*$ ($^3\pi\sigma^*$) and $^3n\pi^*$ states primarily affects the sublevel energies of the bromine containing substituted benzenes. In 4BrBN the T_z and T_x sublevels are lowered by the spin orbit mixing with the $^3\sigma\pi^*$ ($^3\pi\sigma^*$) state, while the T_y and T_x sublevels are lowered by the mixing with the $^3n\pi^*$ state. The spin orbit interaction is given by[1]

$$H_{so} = \sum\xi(l_x s_x + l_y s_y + l_z s_z), \quad (2)$$

where the summation is taken over the electrons. Then the electronic matrix elements which govern the depressions of the sublevel energires due to these mixings are given by

$$\left.\begin{aligned} a &= \frac{|\langle\sigma|\xi l_y|\pi\rangle|^2}{4[E(^3\pi\pi^*)-E(^3\sigma\pi^*)]}\begin{pmatrix}\text{for the mixing with}\\ \text{the } ^3\sigma\pi^* \text{ state}\end{pmatrix}\\ b &= \frac{|\langle n|\xi l_z|\pi\rangle|^2}{4[E(^3\pi\pi^*)-E(^3n\pi^*)]}\begin{pmatrix}\text{for the mixing with}\\ \text{the } ^3n\pi^* \text{ state}\end{pmatrix}\end{aligned}\right\}. \quad (3)$$

If we only consider the one center integrals at the bromine atoms a and b are given by the following expressions.

$$\left.\begin{aligned} a &= \frac{(C^{\sigma}_{Br}C^{\pi}_{Br})^2|\langle p^{Br}_z|\xi 1^{Br}_y|p^{Br}_x\rangle|^2}{4[E(^3\pi\pi^*)-E(^3\sigma\pi^*)]}\\ b &= \frac{(C^{n}_{Br}C^{\pi}_{Br})^2|\langle p^{Br}_y|\xi 1^{Br}_z|p^{Br}_x\rangle|^2}{4[E(^3\pi\pi^*)-E(^3n\pi^*)]}\end{aligned}\right\} \quad (4)$$

Here, C^{σ}_{Br}, C^{n}_{Br}, and C^{π}_{Br} are the coefficients of the bromine atomic orbitals in the σ, n and π molecular orbitals, respectively. ξ is defined by the relation

$$\xi = \frac{1}{4\pi\varepsilon_0}\frac{e^2}{2m^2c^2}\frac{r^3}{Z}, \quad (5)$$

where Z and r are the atomic number of the bromine and the distance of electron from the bromine nucleus, respectively. In the cases of 2BrBN and 3BrBN the z′ and y′ directions are not parallel or perpendicular to the C–Br direction, and both the z′ and y′ sublevels are lowered by the mixings with the $^3\sigma\pi^*$ and $^3n\pi^*$ states. When we take θ as the angle between the y′ axis and the C–Br direction, $T_{z'}$, $T_{y'}$ and $T_{x'}$ sublevels are depressed by $a\cos^2\theta+b\sin^2\theta$, $a\sin^2\theta+b\cos^2\theta$ and $a+b$, respectively. Thus it is convenient to take $\delta=\Delta E_{z'x'}+\Delta E_{y'x'}$ as a measure of the effect of the spin orbit coupling on ZFS. Here ΔE_{ij} are the changes of the energy difference between i and j sublevels on going from the chloro-substituted molecule to the bromo-substituted molecule. δ is equal to $|a+b|$, namely the sum of the contributions due to the mixings with both $^3\sigma\pi^*$ ($^3\pi\sigma^*$) and $^3n\pi^*$ states. These values amount to 0.066 cm^{-1} for the para-substituted benzonitrile in PX, 0.028 cm^{-1} for the ortho- and meta-substituted benzonitriles in the X trap. If we assume that the energy denominators are similar for the para-, ortho-, and meta-substituted molecules, δ are proportional to the spin densities

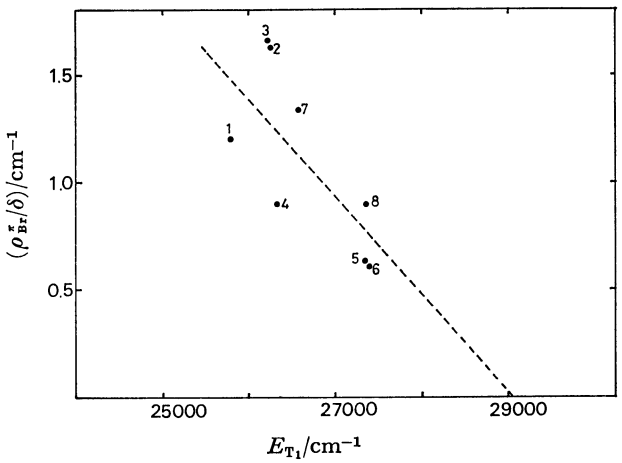

Fig. 3. Plot of ρ^{π}_{Br}/δ *vs.* E_{T_1}; (1) 4-bromobenzonitrile in PX, (2) 4-bromobenzonitrile in DCB, (3) 4-bromobenzonitrile in DBB, (4) 2-bromobenzonitrile X trap, (5) 1,4-dibromobenzene in PX,[7,21] (6) 1-bromo-4-chlorobenzene in PX,[7,21] (7) 4-bromoaniline in PX,[6,22], (8) 4-bromoanisole in PX.[6,22]

on the bromine atom ρ^{π}_{Br}. The observed values of δ are in the order of $\delta(\text{para})>\delta(\text{ortho})\simeq\delta(\text{meta})$ in qualitative agreement with that expected from the spin densities on the bromine $4P_x$ orbitals.

Possible Locations of the Perturbing States. From Eqs. 1—5 we obtain

$$\frac{(C^{\pi}_{Br})^2}{\delta} \propto \frac{1}{\zeta^2}\left\{\frac{(C^{\sigma}_{Br})^2}{E(^3\sigma\pi^*)-E(^3\pi\pi^*)}+\frac{(C^{n}_{Br})^2}{E(^3n\pi^*)-E(^3\pi\pi^*)}\right\}^{-1}. \quad (6)$$

If C^{σ}_{Br} and C^{n}_{Br} do not change much from one molecule to the other, $(C^{\pi}_{Br})^2/\delta$ approaches zero as the perturbing triplet states become close to the T_1 state. In Fig. 3 we plot ρ^{π}_{Br}/δ against the triplet state energy for these systems assuming that $(C^{\pi}_{Br})^2$ is proportional to ρ^{π}_{Br}. ρ^{π}_{Br} were estimated from the bromine hyperfine splittings when the bromine hyperfine splittings were observed. In others they were estimated from the fluorine hyperfine splittings by using the ratio of the fluorine splitting in 4FBN and the bromine splitting in 4BrBN. Though the points are scattered there seems to be a correlation between ρ^{π}_{Br}/δ and the triplet state energy (E_{T_1}) as indicated by the broken line in Fig. 3. The broken line intersects the horizontal axis at $\cong$29000 cm^{-1}. This seems to indicate that there are perturbing states around 29000 cm^{-1}. From the fact that both T_z and T_y sublevels are depressed by the bromine substitution for the para-substituted molecules both $^3\sigma\pi^*$ ($^3\pi\sigma^*$) and $^3n\pi^*$ states are likely to be in the vicinity of 29000 cm^{-1}.

Phosphorescence Spectra and the Main Radiative Mechanisms. The phosphorescence spectra of the representative systems are shown in Fig. 4. The phosphorescence spectra of 4- and 3BrBN, and 4- and 3ClBN in the corresponding xylenes and DCB are well resolved. On the other hand, the resolution of the phosphorescence spectra of 2BrBN and 2ClBN in OX are somewhat poorer, but they still give structures. In the X trap systems which contain small amount of the corresponding xylenes the phosphorescence spectra are broad with some structures. Nevertheless the frequencies of some of the main vibrations observed in the spectrum are similar to those of well resolved one in xylene. Therefore, it is considered that poorly resolved spectra are genuinely due to BrBN and ClBN.

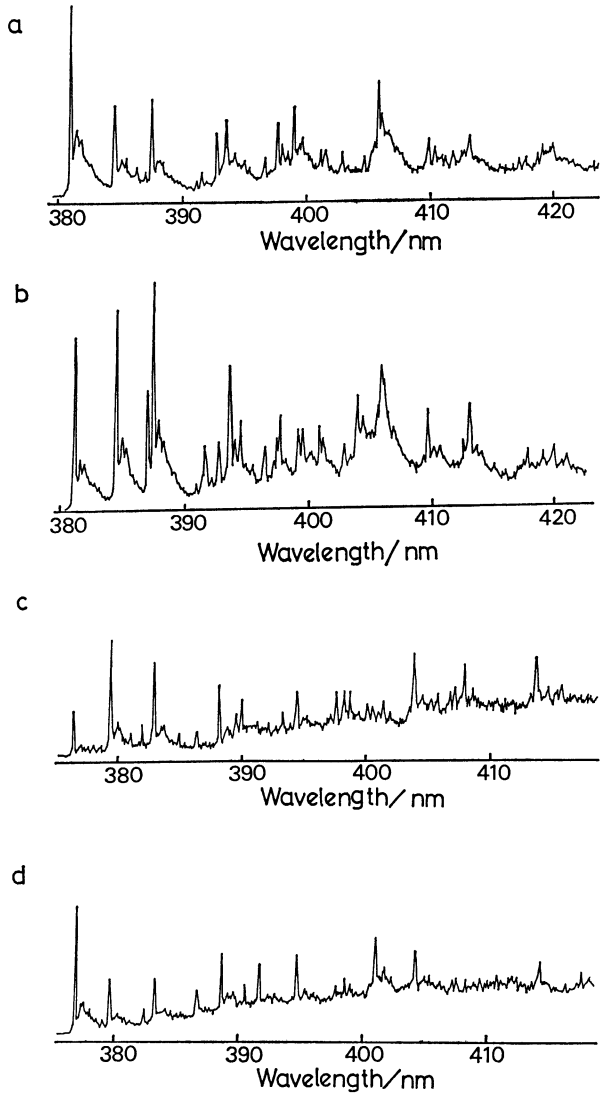

Fig. 4. Phosphorescence spectra of (a) 4-chlorobenzonitrile in DCB, (b) 4-bromobenzonitrile in DCB, (c) 3-chlorobenzonitrile in MX, (d) 3-bromobenzonitrile in MX.

The vibrational analyses of the phosphorescence spectra of 4BrBN and 4ClBN in DCB are given in Table 3. We have made assignments in reference to the infrared and Raman data.[17] In the 4ClBN spectrum the 0-0 band is the strongest. The vibrations of the a_1, b_1, and b_2 symmetries have moderate to weak intensities. On the other hand, in the spectrum of 4BrBN vibrations of the b_1 symmetry are the strongest. The possible mechanisms of the radiative transitions are summarized in Table 4. Since the perturbing states are close to the T_1 state vibronic coupling within the triplet manifold is considered to be dominant. The sublevel spectra of 4BrBN show that the enhanced intensity of the b_1 vibration of

Table 3. Vibrational analysis of the phosphorescence spectrum of 4-chlorobenzonitrile and 4-bromobenzonitrile in DCB at 4.2 K

ν/cm^{-1}	$\Delta\nu$/cm^{-1}	Relative intensity	Assignment	ν/cm^{-1}	$\Delta\nu$/cm^{-1}	Relative intensity	Assignment
4-Chlorobenzonitrile				26007	228	s	b_1
26229		s	(0, 0)	25835	400	m	
25997	242	m	b_1	25806	429	s	b_1
25889	350	w	a_1	25532	703	m	b_1
25836	403	w		25459	776	m	a_1
25801	438	m	b_1	25407	828	s	b_1
25559	681	w		25379	856	w	
25536	703	w		25350	885	m	
25457	782	m	a_1	25228	1006	m	a_1
25408	831	m	b_1	25178	1057	w	a_1
25212	1027	w	a_1	25146	1089	m	b_2
25150	1089	m	a_1	25056	1179	w	a_1
25120	1119	w	b_2	25033	1202	w	
25064	1175	m	a_1	24951	1284	w	b_2
25049	1190	w	a_1	24931	1304	w	
24929	1310	w	b_2	24825	1410	w	b_2
24820	1419	w	b_2	24760	1475	m	a_1
24644	1596	m		24736	1499	w	
24625	1614	w		24642	1593	m	
4-Bromobenzonitrile				24633	1602	w	
26235		s	(0, 0)				

Relative intensity; s>m>w.

Table 4. Main perturbing states for the $^3A_1 \rightarrow {}^1A_1$ radiative transition allowed by group theory

Vibronic band	T_1 sublevel	Spin-orbit	Vibronic-spin-orbit
0, 0	z	$^3A_2(\pi\pi^*) \leftarrow\!\!\sim\!\!\rightarrow {}^1A_2(n\pi^*)$	
a_1	y	$^3B_1(\pi\pi^*) \leftarrow\!\!\sim\!\!\rightarrow {}^1B_1(\sigma\pi^*)$	
	x		
b_1	z		$^3A_2(\pi\pi^*) \leftrightarrow {}^3B_2(\sigma\pi^*) \leftarrow\!\!\sim\!\!\rightarrow {}^1B_2(\pi\pi^*)$
	y		$^3B_1(\pi\pi^*) \leftrightarrow {}^3A_1(\sigma\pi^*) \leftarrow\!\!\sim\!\!\rightarrow {}^1A_1(\pi\pi^*)$
	x		$^3B_2(\pi\pi^*) \leftrightarrow {}^3A_2(\sigma\pi^*) \leftarrow\!\!\sim\!\!\rightarrow {}^1A_2(n\pi^*)$
b_2	z		$^3A_2(\pi\pi^*) \leftrightarrow {}^3B_1(\pi\pi^*) \leftarrow\!\!\sim\!\!\rightarrow {}^1B_1(\sigma\pi^*)$
	y		$^3B_1(\pi\pi^*) \leftrightarrow {}^3A_2(\pi\pi^*) \leftarrow\!\!\sim\!\!\rightarrow {}^1A_2(n\pi^*)$
	x		$^3B_2(\pi\pi^*) \leftrightarrow {}^3A_1(\pi\pi^*) \leftarrow\!\!\sim\!\!\rightarrow {}^1A_1(\pi\pi^*)$
a_2	z		$^3A_2(\pi\pi^*) \leftrightarrow {}^3A_1(n\pi^*) \leftarrow\!\!\sim\!\!\rightarrow {}^1A_1(\pi\pi^*)$
	y		$^3B_1(\pi\pi^*) \leftrightarrow {}^3B_2(n\pi^*) \leftarrow\!\!\sim\!\!\rightarrow {}^1B_2(\pi\pi^*)$
	x		$^3B_2(\pi\pi^*) \leftrightarrow {}^3B_1(n\pi^*) \leftarrow\!\!\sim\!\!\rightarrow {}^1B_1(\sigma\pi^*)$

State symbols give the total symmetries.

4BrBN is mainly due to the T_y sublevel emission. Then the importance of the spin orbit vibronic mechanism involving $^3\pi\pi^* \leftrightarrow {}^3\sigma\pi^*$ ($^3\pi\sigma^*$) vibronic coupling increases on going from 4ClBN to 4BrBN (Fig. 5).

In the case of the meta-substituted benzonitrile the 0-0 band is stronger in the bromo-substituted molecule than in the chloro-substituted molecule. This indicates that the relative importance of the mechanism involving the $^1\sigma\pi^*$ ($^1\pi\sigma^*$) state increases on going from the chloro-substituted molecule to the bromo-substituted molecule.

In spite of the poor molecular symmetry of 3BrBN the $T_{y'}$ and $T_{x'}$ sublevel spectra are very different (Fig. 6). If we assume that only one center integral at the bromine atom is important in determining the radiative decay, this observation implies that the directions of the z′ and y′ axes are either nearly parallel or perpendicular to the C–Br direction. This result is in agreement with the conclusion obtained from the analysis of hfs and ZFS that the halogen substitution at the meta position perturbs the spin distribution of the present molecule greately.

Nuclear Charge and Position Dependence of the Decay Rates. We measured the total and relative radiative decay rate constants of the sublevels by the technique of microwave induced delayed phosphorescence (MIDP). The decay properties of the halogen-substituted benzonitriles are summarized in Table 5. The decay rate constants obtained in methylcyclohexane glass at 77k are also shown in Table 5. In order to study the position dependence of the decay rates we use $k_{av}=1/2(k_{y'}+k_{z'})$, because many molecules

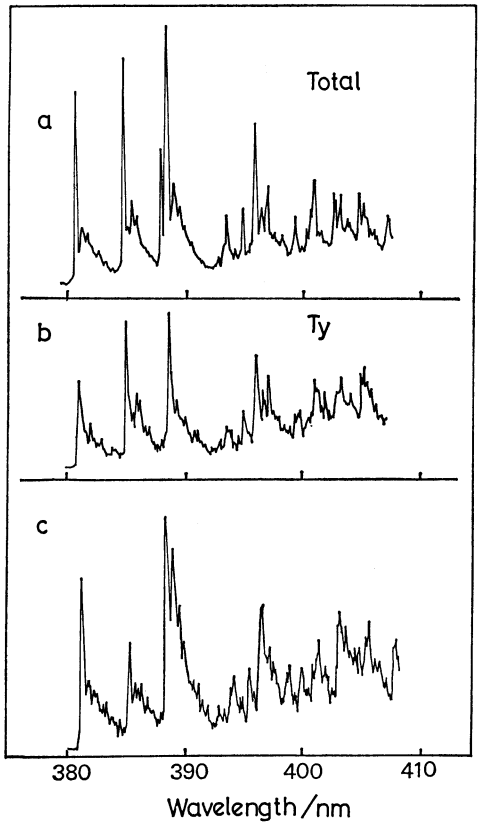

Fig. 5. MIDP and time resolved spectra of 4-bromobenzonitrile in DCB.
(a) Total phosphorescence spectrum. (b) MIDP spectrum obtained by the application of microwave at 4.1 GHz. (c) Time resolved spectrum obtained at 10 ms after excitation.

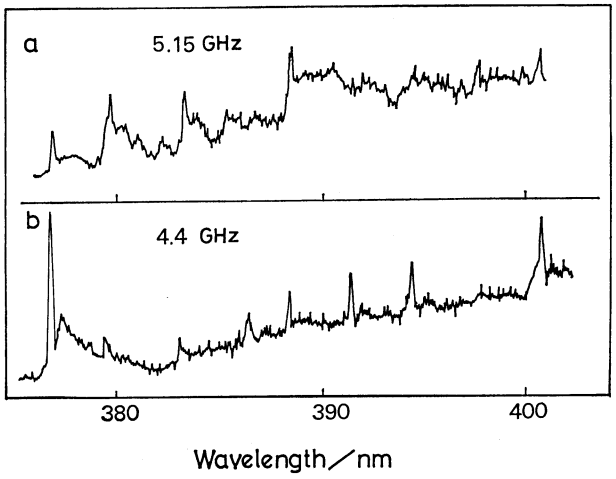

Fig. 6. MIDP spectra of 3-bromobenzonitrile in MX, (a) obtained by the application of microwave at 5.15 GHz, (b) obtained by the application of microwave at 4.4 GHz.

do not have C_{2v} symmetry and it is not possible to discuss the heavy atom effect on k_z' and k_y' seperately. Important results concerning the nuclear charge and position dependence may be summarized in the following.

(1) In the cases of the para-substituted benzonitrile the nuclear charge dependence is very dependent on the sublevel. $k_y(\mathrm{Br})/k_y(\mathrm{Cl})$ are 88 and 52 in PX and DCB host, respectively. These values are much larger than $\zeta^2_{\mathrm{Br}}/\zeta^2_{\mathrm{Cl}}$. On the other hand, $k_z(\mathrm{Br})/k_z(\mathrm{Cl})$ are only 22 and 11 in PX and DCB, respectively. $k_x(\mathrm{Br})/k_x(\mathrm{Cl})$ is also relatively small.

(2) $k_{av}(\mathrm{Br})/k_{av}(\mathrm{Cl})$ are 58, 35, and 35 for the para-substituted benzonitrile in PX, in DCB and in methylcyclohexane, 30 and 33 for the meta-substituted one in MX and in methylcyclohexane, and 38 and 34 for the ortho-substituted one in OX and in methylcyclohexane. These values are also substantially larger than those found for other systems (for 1- and 2-halonaphthalene in EPA glass these values are 20.9 and 21.4, respectively), though they depend on the host. The nuclear charge dependences are shown schematically in Fig. 7.

Table 5. Dynamic properties of halogen containing benzonitriles

Molecule		$k^{a)}$ / s^{-1}	$k^{r}(00)^{b)}$	$k_{av}^{c)}$ / s^{-1}	$k_{av}^{d)}$ / s^{-1}
4BrBN (in PX)[f]	z	110	10		
	y	580	25	345	352
	z	3.9	1		
(in DCB)	z	85			
	y	540		313	
	x	4.9			
3BrBN (in MX)	z′	190			
	y′	89	30	140	145
	x′	6.5	1		
(MX doped)	z′	92	13		
	y′	110	39	101	
	x′	5.1	1		
2BrBN (in OX)	z′				
	y′			184[e]	165
	x′				
(OX doped)	z′	130	13		
	y′	75	11	103	
	x′	3.7	1		
4ClBN (in PX)[f]	z	5.0	13.5		
	y	7.0	25	6.0	10.0
	x	0.28	1		
(in DCB)	z	7.6			
	y	10.4		9.0	
	x	0.52			
(PX doped)	z	3.2			
	y	19.6		11.0	
	x	0.30			
3ClBN (in MX)	z′				
	y′			4.5[e]	4.4
	x′				
2ClBN (in OX)	z′				
	y′			4.9[e]	4.8
	x′				
4FBN					0.85
3FBN					0.65
2FBN					0.73

a) Total decay rates. b) Relative radiative decay rates obtained at the 0-0 band. c) $k_{av}=1/2(k_y+k_z)$ or $1/2(k_{y'}+_{z'})$ except where indicated. d) $k_{av}=1/2(k_{x'}+k_{y'}+k_{z'})$ in methylcyclohexane at 77 K. e) $k_{av}=1/2(k_{x'}+k_{y'}+k_{z'})$. f) Taken from Ref. 6.

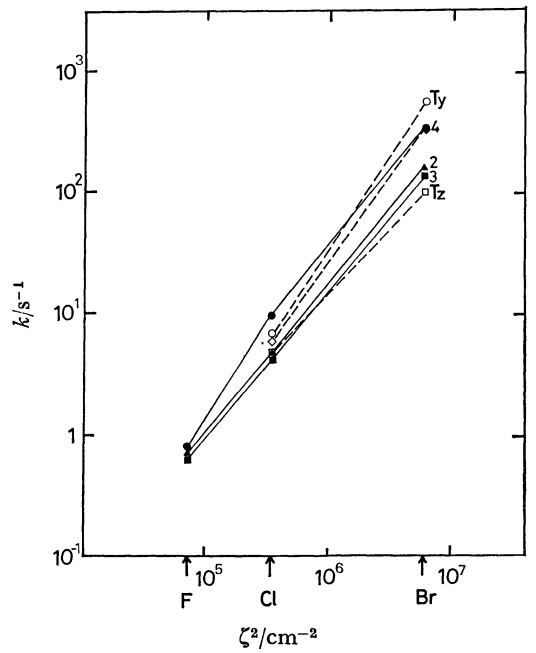

Fig. 7. Nuclear charge and position dependences of the decay rates.
●: k_{av} of the para-substituted molecules, ▲: the ortho-substituted ones, ■: the meta-substituted ones in methylcyclohexane. ◇: k_{av}, ○: T_y sublevel decay rate, □: T_z sublevel decay rate of the para-substituted ones in *p*-xylene.

(3) k_{av} are in the following order, $k_{av}(\text{para})>k_{av}(\text{ortho})>k_{av}(\text{meta})$. Although the decay rate constants depend on the host considerably, k_{av}(para) are 2—3 times larger than k_{av}(ortho) and k_{av}(meta).

We discuss these results based on the factors which govern the radiative and nonradiative decay rates. The transition moment $\boldsymbol{M}(T_1\rightarrow S_0)$ between the T_1 state and the ground state is given by[18]

$$\boldsymbol{M}(T_1\rightarrow S_0) = \sum_k \frac{1}{E^0(T_1)-E^0(S_k)}\left\{\langle S_k|H(1)|T_1\rangle + \sum_n \frac{\langle S_k|H(2)|S_n\rangle\langle S_n|H(1)|T_1\rangle}{E^0(T_1)-E^0(S_n)} + \sum_{n\neq 1} \frac{\langle S_k|H(1)|T_n\rangle\langle T_n|H(2)T_1\rangle}{E^0(T_1)-E^0(T_n)}\right\}\langle S_k|\Sigma e\boldsymbol{r}_i|S_0\rangle, \quad (7)$$

where $H(1)=H_{so}^{(0)}$, $H(2)=\sum_k(\partial H_0/\partial Q_k)Q_k$, and Q_k are the normal vibrational coordinates of the given electronic state. The first term inside the parentheses gives the transition at the electronic origin induced by the direct spin orbit coupling, while the second and the third terms embody the vibronic spin orbit mechanisms. In the present systems $^3\sigma\pi^*$ ($^3\pi\sigma^*$) and $^3n\pi^*$ states are close to the T_1 state and the vibronic interactions involving these states are considered to be dominant. The important singlet states which couple with the $T_1(\pi\pi^*)$ state are $^1\sigma\pi^*$ and $^1n\pi^*$ states. The matrix elements such as $\langle^1\sigma\pi^*|H_{so}|^3\pi\pi^*\rangle$ and $\langle^1n\pi^*|H_{so}|^3\pi\pi^*\rangle$ are reduced to $C_h^\sigma C_h^\pi\langle P_z^h|\xi l_y^h|P_x^h\rangle$ and $C_h^n C_h^\pi\langle P_y^h|\xi l_z^h|P_x^h\rangle$, when only one center integrals at the halogen atoms are taken into consideration. Here, C_h^π, C_h^σ, and C_h^n are the AO coefficients of the halogen atomic orbitals which constitute the π, σ and n orbitals. Similar expressions are obtained for the spin orbit couplings between the $^1\pi\pi^*$ state and $^3\sigma\pi^*$ and $^3n\pi^*$ states.

In the case of nonradiative decay we use the expression for nonradiative transition obtained by Metz *et al.*;[19] the pure spin Born-Oppenheimer functions are used as a zeroth order basis set,[20] the dominant perturbation is assumed to be the spin orbit coupling operator, and the electronic transition moment is expanded about the equilibrium nuclear configuration of the ground state, *viz.*,

$$\langle T_1|H_{so}|S_0\rangle = \langle T_1^0|H_{so}|S_0^0\rangle + \sum_{j,k}\{(E_{S_0}^0-E_{S_j}^0)^{-1}[\langle T_1^0|H_{so}|S_j^0\rangle\langle S_j^0|H_{vib}|S_0^0\rangle]_0Q_k\} + \sum_{m,k}\{(E_{T_1}^0-E_{T_m}^0)^{-1}[\langle T_1^0|H_{vib}|T_m^0\rangle\langle T_m^0|H_{so}|S_0^0\rangle]_0Q_k\}. \quad (8)$$

Here the superscript zeros denote the zeroth order wave functions and energies, the subscript zeros denote the reference configuration, H_{vib} is the vibronic coupling operator and Q_k are the normal coordinates describing the displacements from the reference configuration. We neglect spin vibronic term.

The first term in Eq. 8 is vanishingly small for planar conformation because of $\pi\pi^*$ character of the T_1 state. The spin orbit matrix elements in the second and third terms in Eq. 8 depend on the coefficients of the halogen atomic orbitals as in the case of the radiative decay. The dependence of the spin orbit matrix elements on the coefficients of the halogen atomic orbitals and the relevant energy denominators for the radiative and nonradiative transitions are given in Table 6.

In the present approach the decay rate constants depend on the energy denominator, AO coefficient of the halogen atomic orbital, the matrix element for the vibronic interaction, the transition moments for $S_0\rightarrow S_k$ transitions involved in the main decay mechanisms, and the spin orbit coupling constant ζ. If the factors other than ζ do not change on going from the chloro-substituted molecule to the bromo-substituted molecule, the decay rate constants would be approximately proportional to ζ^2. Since the extent of the spin delocalization into the halogen atom increases on going from fluorine to iodine, the increase in the decay rate may be somewhat larger than expected from ζ^2. When we take account of this increase, the ratio of the spin orbit coupling matrix elements for bromine and chlorine is 24.4. The values observed for naphthalene and phenanthrene are indeed close to this value.[14] In these systems the above condition may be satisfied.

Since different sublevels couple with different perturbing states, the heavy atom enhancement is in principle sublevel dependent. In 4BrBn the enhancement was found to be much larger for the T_y sublevel decay than for the T_z sublevel decay. The T_y sublevel decay is mostly due to the mechanisms involving the vibronic interaction between the T_1 state and the $^3\sigma\pi^*$ ($^3\pi\sigma^*$) state. The larger value of k_y(Br)/k_y(Cl) seems to imply that the energy denominator for the $^3\sigma\pi^*$ ($^3\pi\sigma^*$) state substantially decreases on going from 4ClBN to 4BrBN. On the other hand

Table 6. The radiative and nonradiative decay mechanisms, relevent spin orbit matrix elements and energy denominators

	Decay mechanism	Spin-orbit matrix element[b]	Energy denominator
Radiative decay			
spin-orbit	$^3\pi\pi^* \longleftrightarrow {}^1\sigma\pi^*$	$C_h^x C_h^z \langle P_x^h \vert \xi 1_{y'}^h \vert P_{z'}^h \rangle$	$\Delta E(^1\sigma\pi^* - {}^3\pi\pi^*)$
	$^3\pi\pi^* \longleftrightarrow {}^1n\pi^*$ [a]	$C_h^z C_h^n \langle P_x^h \vert \xi 1_{z'}^h \vert P_{y'}^h \rangle$	$\Delta E(^1n\pi^* - {}^3\pi\pi^*)$
vibronic-spin-orbit	$^3\pi\pi^* \longleftrightarrow {}^3\sigma\pi^* \longleftrightarrow {}^1\pi\pi^*$	$C_h^z C_h^x \langle P_{z'}^h \vert \xi 1_{y'}^h \vert P_x^h \rangle$	$\Delta E(^1\pi\pi^* - {}^3\pi\pi^*) \times \Delta E(^3\sigma\pi^* - {}^3\pi\pi^*)$
	$^3\pi\pi^* \longleftrightarrow {}^3n\pi^* \longleftrightarrow {}^1\pi\pi^*$	$C_h^n C_h^x \langle P_{z'}^h \vert \xi 1_{y'}^h \vert P_x^h \rangle$	$\Delta E(^1\pi\pi^* - {}^3\pi\pi^*) \times \Delta E(^3\sigma\pi^* - {}^3\pi\pi^*)$
	$^3\pi\pi^* \longleftrightarrow {}^3\pi\pi^* \longleftrightarrow {}^1\sigma\pi^*$	$C_h^z C_h^x \langle P_x^h \vert \xi 1_{y'}^h \vert P_{z'}^h \rangle$	$\Delta E(^1\sigma\pi^* - {}^3\pi\pi^*) \times \Delta E(^3\pi\pi^* - {}^3\pi\pi^*)$
	$^3\pi\pi^* \longleftrightarrow {}^3\pi\pi^* \longleftrightarrow {}^1n\pi^*$	$C_h^z C_h^n \langle P_x^h \vert \xi 1_{z'}^h \vert P_{y'}^h \rangle$	$\Delta E(^1n\pi^* - {}^3\pi\pi^*) \times \Delta E(^3\pi\pi^* - {}^3\pi\pi^*)$
Nonradiative decay			
	$^3\pi\pi^* \longleftrightarrow {}^3\sigma\pi^* \longleftrightarrow G$	$C_h^{z*} C_h^z \langle P_x^h \vert \xi 1_{y'}^h \vert P_{z'}^h \rangle$	$\Delta E(^3\sigma\pi^* - {}^3\pi\pi^*)$
	$^3\pi\pi^* \longleftrightarrow {}^3n\pi^* \longleftrightarrow G$	$C_h^{z*} C_h^n \langle P_x^h \vert \xi 1_{z'}^h \vert P_{y'}^h \rangle$	$\Delta E(^3n\pi^* - {}^3\pi\pi^*)$
	$^3\pi\pi^* \longleftrightarrow {}^1\sigma\pi^* \longleftrightarrow G$	$C_h^z C_h^z \langle P_x^h \vert \xi 1_{y'}^h \vert P_{z'}^h \rangle$	$\Delta E(^1\sigma\pi^* - G)$
	$^3\pi\pi^* \longleftrightarrow {}^1n\pi^* \longleftrightarrow G$	$C_h^z C_h^n \langle P_x^h \vert \xi 1_{z'}^h \vert P_{y'}^h \rangle$	$\Delta E(^1n\pi^* - G)$

a) Only for meta and orhto substituted molecules. b) The x axis is perpendicular to the molecular plane, the z′ axis is parallel to the C–Br direction, and the y′ axis is perpendicular to the other two.

the energy denominator for the $^3n\pi^*$ state may not change much.

The increase of the T_y sublevel decay rate because of the reduction in the energy denominator seems to be manifested in the large change of the T_y sublevel decay rate on going from 1-bromonaphthalene[9] through 4BrBN to 1-bromo-4-chlorobenzene.[7] The decay rate constants are 159 s^{-1}, 580 s^{-1}, and 1540 s^{-1}, respectively following the order of the T_1 state energy. The $^3\sigma\pi^*$ ($^3\pi\sigma^*$) state should be very close to the T_1 state of 1-bromo-4-chlorobenzene as also indicated by the analysis of ZFS.[7]

When the increase of the $T_{y'}$ sublevel decay rate is much larger than that expected from ζ^2, $k_{av}(Br)/k_{av}(Cl)$ also becomes larger than that expected from ζ^2. $k_{av}(Br)/k_{av}(Cl)$ of the ortho- and meta-substituted benzonitrile are also considerably larger than expected from ζ^2 as in the case of para-substituted benzonitrile. This is expected when the decay mechanism involving the $^3\sigma\pi^*$ ($^3\pi\sigma^*$) state is dominant as in the case of 4BrBN.

The present analysis shows that the relationship between the decay rate and the spin density is not so straightforward, because the decay rate is determined by a number of factors. When the T_1 state is approximated by the single excitation from the HOMO (π) to the LUMO (π^*), the spin density on the halogen atom is given by $|C_h^H|^2 + |C_h^L|^2$. Here C_h^H and C_h^L denote the AO coefficients of halogen in the HOMO and the LUMO, respectively. The radiative decay rate depends on $|C_h^H|^2$. If the π^* orbital relevant to the spin orbit matrix elements governing the nonradiative decay is the LUMO, the nonradiative decay rate depends on $|C_h^L|^2$ and $|C_h^H|^2$. Therefore, a qualitative correlation between the spin density on the halogen atom and the decay rate may be obtained as observed in phenanthrene, if other factors such as energy denominators remain the same. In the present systems, $k_{av}(para) \simeq 2k_{av}$ (ortho) also correlates well with $\rho_{Br}(para \simeq 3\rho_{Br}$ (ortho). In spite of the complexities of the factors governing the decay rates, the correlation between the decay rate and the spin density may not be uncommon.

References

1) S. P. McGlynn, T. Azumi, and M. Kinoshita, "Molecular Spectroscopy of Triplet State," Prentice Hall, Englewood Cliffs, N. J. (1969), Chap. 7.
2) D. S. McClure, *J. Chem. Phys.*, **17**, 905 (1949).
3) S. P. McGlynn, R. Sunseri, and N. Christodouleas, *J. Chem. Phys.*, **37**, 1818 (1962).
4) J. C. Miller, J. S. Meek, and S. J. Strikler, *J. Am. Chem. Soc.*, **99**, 8175 (1977).
5) F. Masetti, U. Mazzucato, and G. Galuazzo, *J. Lumin.*, **4**, 8 (1971).
6) S. Niizuma, L. Kwan, and N. Hirota, *Mol. Phys.*, **35**, 1029 (1978).
7) H. Shinohara and N. Hirota, *J. Chem. Phys.*, **72**, 4445 (1980).
8) G. Kothandraman, H. J. Yue, and D. W. Pratt, *J. Chem. Phys.*, **61**, 2102 (1974).
9) H. Saigusa and T. Azumi, *J. Chem. Phys.*, **71**, 1408 (1979).
10) N. Hirota, T. C. Wong, E. T. Harrigan, and K. Nishimoto, *Mol. Phys.*, **29**, 903 (1975).
11) T. H. Cheng and N. Hirota, *Mol. Phys.*, **27**, 281 (1974).
12) Y. Asahi and N. Hirota, *Mol. Phys.*, **41**, 1211 (1980).
13) J. Mispelter, J.-Ph, Grivet, and J. M. Lhoste, *Mol. Phys.*, **21**, 999 (1971).
14) A. M. P. Goncalves and C. A. Hutchison, Jr., *J. Chem. Phys.*, **54**, 2962 (1971).
15) C. R. Jones, A. H. Maki, and D. R. Kearns, *J. Chem. Phys.*, **59**, 873 (1973).
16) H. Hayashi and S. Nagakura, *Mol. Phys.*, **24**, 801 (1972).
17) J. H. S. Green and D. J. Harrison, *Spectrochim. Acta*, **32**, 1279 (1976).
18) E. C. Lim, "Excited States," ed by E. C. Lim, Academic, New York (1977), Vol. 3, Chap. 5.
19) F. Metz, S. Friedrich, and G. Hohlneiher, *Chem. Phys. Lett.*, **16**, 353 (1972).
20) B. R. Henry and W. Siebrand, *J. Chem. Phys.*, **54**, 1072 (1971).
21) In the cases of 1-bromo-4-chlorobenzene and 1,4-dibromobenzene, the spin densities on the bromine were assumed to be proportional the spin densities on carbon 4 (0.33).
22) Y. Asahi and N. Hirota, *Mol. Phys.*, in press.